



Observation of three-dimensional behavior in surface states of bismuth nanowires and the evidence for bulk-Bi surface quasiparticles

T. E. Huber,¹ A. Nikolaeva,² L. Konopko,² and M. J. Graf³

¹Howard University, Washington, DC 20059-0001, USA

²Academy of Sciences of Moldova, Chisinau, MD 2028, Moldova and International Laboratory of High Magnetic Fields and Low Temperatures, 53-421 Wrocław, Poland

³Department of Physics, Boston College, Chestnut Hill, Massachusetts 02467, USA

(Received 16 March 2009; published 13 May 2009)

We studied trigonal Bi nanowires ($30 \text{ nm} < \text{diameter} < 200 \text{ nm}$) via low-temperature magnetotransport for fields up to 14 T in order to investigate the role of their surfaces. A two-dimensional behavior was expected; we found instead a three-dimensional behavior, with a rich spectrum of Landau levels in a nearly spherical Fermi surface. We show that recent observations of sharp peaks in the bulk-Bi Nernst thermopower near the 9 T quantum limit attributed to charge fractionalization, can be more plausibly interpreted in terms of surface states. Bismuth has a true quantum limit at around 70 T.

DOI: [10.1103/PhysRevB.79.201304](https://doi.org/10.1103/PhysRevB.79.201304)

PACS number(s): 73.21.Hb, 68.35.-p, 71.70.Di

Bi has a Fermi surface (FS) consisting of small hole and electron pockets at T and L points, respectively, [Fig. 1(a)], and therefore the Fermi wavelength λ_F is very long (about 50 nm). The magnetic energy, which is inversely proportional to λ_F , is sufficiently large in comparison with the Fermi energies to depopulate Bi of holes in magnetic fields (H) as small as 9 T. The high- H state has been studied experimentally¹ and the results were well described by the model of holes and Dirac electrons with strong spin-orbit interaction.² Therefore, the interpretation by Behnia *et al.*³ of their measurements of Nernst thermopower and Hall effect of bulk Bi in terms of charge fractionalization (a collective quantum state) was unexpected because it would involve new quasiparticles. Subsequently, Li *et al.*⁴ presented a study of the magnetic properties that was largely confirmatory of Ref. 3 in this regard. Clearly, the observation in bulk Bi of two-dimensional (2D) quantum phenomena,⁵ as observed in 2D electron gases, is very exciting.⁶ But Refs. 3 and 4 do not address the main issues raised by their interpretation, that is, what is the nature of the quasiparticles and the origin and dimensionality of the phase underlying the effect.

Because electrons and holes in bulk Bi exhibit very long relaxation times, the electronic mean-free path in bulk Bi is several millimeters long,⁷ significantly longer than the size of the samples in the experiments. The diffusion thermopower expressions do not apply, rather it can be presumed that the boundary plays an important role in the energy relaxation of the charge carriers. Since the thermoelectric potentials, as well as the electric potentials associated with wrapping (surface) currents, are determined by relaxation processes,⁸ surface relaxation effects will play a key role in low-temperature experiments involving Bi, and, in particular, in the experiments in Refs. 3 and 4. Direct observations via angle-resolved photoemission spectroscopy (ARPES) show that semi-infinite Bi surfaces support a large density of surface states that are populated by electrons of density $\Sigma \sim 2-5 \times 10^{12} \text{ cm}^{-2}$, effective mass $m_\Sigma \sim 0.2$.⁹ By applying ARPES to ultrathin Bi films, Hirahara *et al.*¹⁰ provided evidence of the bulklike (BL) states and boundary states in Bi and argued that they are hybridized. Hybridization could be a

primary mechanism for energy relaxation of bulk carriers. However, ARPES measurements in Ref. 10 did not measure transport properties or the effect of magnetic fields, and therefore the connection between relaxation processes and the results of Refs. 3 and 4 is not clear. Here, we report magnetotransport measurements in high mobility 30-, 50-, and 200-nm-diameter Bi nanowire arrays, for which we observe a spectrum of resonances of bulklike quasiparticles and surface carriers as a function of magnetic field up to 16 T. Our results directly address the role of the boundary in the transport properties of solid samples. Preliminary studies have been presented.^{11,12} Because of their special periodicity in $1/H$, we argue that we observe resonances that are caused by Landau states (LSs) in a spherical Fermi surface formed in the body of the nanowires from the penetrating surface

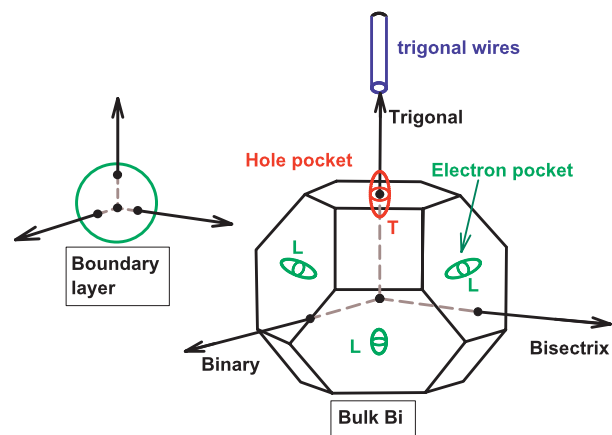


FIG. 1. (Color) Fermi surfaces of the bulk and the boundary layer of bismuth. Bulk: it shows the spatial distribution, with respect to the Brillouin zone, of the wave vectors of L electrons and T holes whose energies are at the Fermi level. The crystalline orientation of the trigonal nanowires is shown. In these nanowires, the three electron pockets are crystallographically equivalent. Boundary layer: the spherical Fermi surface of the boundary charges in the present Rapid Communication.

states in the nanowire boundary. We contend that the nanowires still exhibit the same physics that semi-infinite surfaces do because our observed spectrum of resonances (the location of the peaks as a function of $1/H$) of the boundary's LS and the resonances observed by Behnia are remarkably similar. This then calls into question the interpretation of results in terms of fractionalization presented in Ref. 3.

Depending upon the diameter d , nanowires may present extreme behaviors because of quantum confinement effects¹³ and their large surface-to-volume ratio. While the LS spectrum of electrons and holes in the large-diameter nanowires—apart from small quantum confinement shifts—is analogous to that for bulk Bi, and the electrons and holes are the majority carriers, the very small-diameter nanowires ($d < \lambda_F$) realize the quantum limit without magnetic fields. For these nanowires, the quantum confinement energy $E_c = \hbar^2 \pi^2 / 2m^* m_e d^2$, where m_e is the electron mass and m^* is the effective mass in units of m_e , exceeds the electron-hole overlap energy E_0 . Therefore, electron n and hole p densities are decreased critically below the bulk equilibrium values ($n_0 = p_0 = 3 \times 10^{17} \text{ cm}^{-3}$), resulting in a semimetal (SM)-to-semiconductor (SC) (SMSC) transition.¹⁴ The SMSC critical diameter for holes and electrons for our nanowires ($m^* = 0.065$) is around 50 nm. Accordingly, it is expected that 30 nm wires are SC, 200 nm wires are SM, and 50 nm wires are at the SMSC. The argument for the SMSC neglects surface states. Given the reduction in the bulk electron n and hole p densities relative to the surface carrier concentration Σ , one expects the surface carriers to become a clear majority in nanowires with diameters below 100 nm at low temperatures; for example, the ratio of surface carriers per unit length to bulk electrons or holes per unit length is 15 for 50 nm wires. This ratio is even larger for nanowires on the SC side of the SMSC transition.

We employ high mobility intrinsic nanowire samples, namely, arrays of trigonal nanowires [the orientation is shown in Fig. 1(a)] of diameters ranging between 30 and 200 nm prepared by the high-pressure infiltration of pure Bi (99.999%) into nanochannel alumina templates.¹¹ Our two-probe electrical contact technique consists of attaching Cu wire electrodes to both sides of the Bi nanowire composite by using silver epoxy contacts. We will show below that these samples support LS. The LS levels inverse-field oscillatory period is $\Delta(1/H) = e/(cA_e)$, where A_e is any extremal cross-sectional area of the Fermi surface perpendicular to the magnetic field.¹⁵ For an ellipsoidal FS, the carrier density is $p = (1/3\pi)A_{\perp}A_{\parallel}^{1/2}$ where \parallel and \perp refer to the directions along the major and minor axes. The effective mass m^* (dA/dH) and relaxation time can be extracted from the oscillatory magnetoresistance (MR). 1.8-K-MR measurements were made in two separate laboratories: (i) Boston College for $H < 9$ T and (ii) International Laboratory of High Magnetic Fields and Low Temperatures (Wroclaw, Poland) for $H < 14$ T, employing a cryostat which allowed for *in situ* sample rotation around two axes. This made possible the measurement of the longitudinal MR (LMR), transverse MR (TMR), and measurements at intermediate orientations θ of the nanowires with respect to the magnetic field; the mesh was limited to 15° due to magnet time limitations. In order to successfully interpret LS data for small-diameter nanowires,

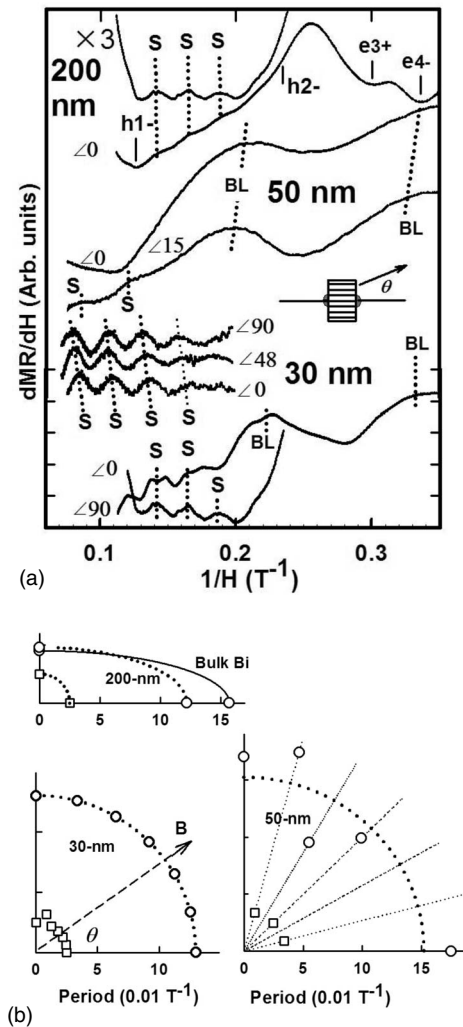


FIG. 2. Top: angle-dependent derivative of the magnetoresistance of Bi wire array samples of various diameters as indicated. Inset: schematic view of the nanowire array sample with silver epoxy contact; the magnetic field is represented as an arrow at an angle θ with respect to the wire lengths. Bottom: polar plot of the SdH periods of holes (circles) in bulk Bi and assigned to S (squares) and BL (circles) quasiparticles in 200-nm, 50-nm, and 30-nm-nanowire samples. The dotted arcs are provided as guide for the eyes where appropriate. The symmetry, spherical, or ellipsoidal of these plots reflects the symmetry of the corresponding Fermi surfaces.

one needs to consider the electronic transport regime (ballistic versus diffusive) and Chambers's effect.¹⁶ The Chambers magnetic field H_c is that for which the Larmor radius $r_L = \hbar c k_F / |e|H$ is less than $d/2$. Here, k_F is the actual Fermi wave vector, \hbar is Planck's constant, c is the speed of light, and e is the electronic charge. For high-purity samples, it is expected that $\text{LMR} < \text{TMR}$ when $H > H_c$ because at high magnetic fields, the carriers avoid collision with the walls when the magnetic field is oriented along the wire direction. Our samples indeed satisfy this condition.

Figure 2 (top) shows the high- H , $d(\text{MR})/dH$ versus $1/H$ for the nanowires in our study at low temperatures at some

illustrative orientations. The sequences indicated by S and BL are the main motivation for the present Rapid Communication. The short-period S sequence was not observed in bulk-Bi resistance but was observable in 200 nm wires and was strong in the finer nanowires. Also, the period of the S sequence is roughly independent of diameter. These facts suggest that S states have a surface origin. However, the S sequence is observed in the LMR case, where the magnetic field is perpendicular to the boundaries. A planar (2D) electron gas simply would not have Landau states in this case because the orbits enclose no flux. In 200 nm nanowires, the S peaks occur together with electrons and holes peaks. The strong LMR peaks at 0.125 T^{-1} , at the end of our observation range (9 T) is the h_1^- , the singlet at the hole quantum limit (there are no hole LS eigenstates at higher magnetic fields). The peak indexed h_2^- is the $2^-, 0^+$ hole doublet. It is observed at 0.255 T^{-1} in 200-nm-Bi nanowires and at 0.22 T^{-1} in bulk Bi.¹⁷ The modest shift of 0.02 T^{-1} can be interpreted in terms of quantum confinement; m^* is observed not to be modified by confinement. Electron features are also observed as seen in the figure. g is not modified substantially for electrons and holes; i.e., it is observed that the hole spin splitting is almost twice the Landau-level spacing as in the bulk. Results are summarized in Fig. 2, at the bottom, showing that the FS of holes in 200 nm nanowires displays the characteristic ellipsoidal anisotropy of bulk Bi but with an eccentricity A_\perp/A_\parallel that is less than that in the bulk. In the 50 and 30 nm wires, the sharp (h) hole features are not observed and the S sequence is instead paired with the long-period sequence that we identify as BL states. The values of the effective masses confirm our assignment. For the 30 nm S states and BL states, we find $m_S^* \sim 0.3$ and $m_{BL}^* \sim 0.06$, respectively. Our observation of a large effective mass for the S sequence, comparable to the surface-states effective mass m_Σ , leads us to conclude that it is associated with the surface states observed with ARPES. In contrast, the small effective mass extracted for the BL sequence is consistent with bulk-like carriers that have been modified by quantum confinement effects.

In 30 nm wires, the S sequences show an isotropic Shubnikov-de Haas (SdH) period of 0.025 T^{-1} , consistent with spherical pockets of the Fermi surface of density $n_S = (1.3 \pm 0.2) \times 10^{18}/\text{cm}^3$. LS extend over the $r_L = 17 \text{ nm}$ when $B = 5 \text{ T}$. Therefore, the S states in 30 nm nanowires fill a very significant fraction of the 30-nm-diameter wire which can no longer be considered a 2D cylindrical conductor covered by boundary charges. This three-dimensional (3D) behavior contrasts with the 2D behavior related to the short penetration length of surface states observed in binary nanowires, whose crystalline orientation is perpendicular to the trigonal axis.¹⁸

A number of semi-infinite surfaces was studied using ARPES. States that have relatively high-effective masses and similar carrier densities are found on all low-index surfaces studied so far.⁹ ARPES measurements also show that the surface states are essentially 2D; however the penetration length, is very anisotropic. "It is known that the (100) surface supports deeply penetrating states in contrast to trigonal surfaces, where the surface states are shallow." It is conceivable that the deeply penetrating surface states form a base for

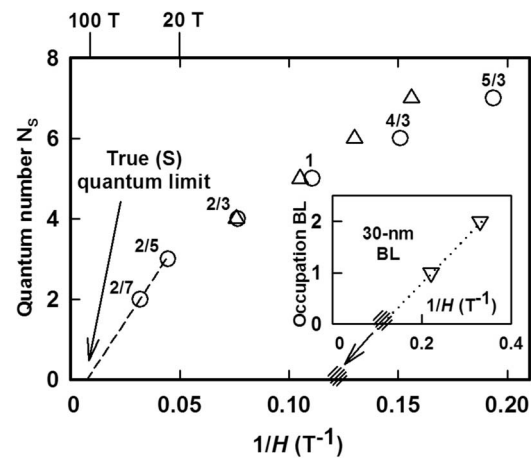


FIG. 3. Circles: Points in Behnia *et al.* (Ref. 3) that were interpreted in terms of fractionalization; the fractions are indicated. Instead of designating the points as fractional, we assign them a sequential integral index N_S . The dashed line shows the extrapolation that gives a surface-states quantum limit of 70 T. Up triangles: boundary Landau states data of 30-nm-Bi nanowires. Inset: bulklike Landau states data (down triangles) of 30 nm nanowires.

the LS. The surface charge per unit area σ can be estimated as $n_S \times r_L$, which we find to be $\sigma = 2.2 \times 10^{12}/\text{cm}^2$ in rough agreement with the Σ determined via ARPES measurements.⁹ We also find that $n_{BL} = (1.0 \pm 0.5) \times 10^{17}/\text{cm}^3$. Therefore, $n_{BL} \sim 1/3 n_0$ even though the 30 nm nanowires are on the SC side of the SMSC transition ($E_c > E_0$). We will address this result below. As is shown by the polar plots of the SdH periods, 30 nm nanowires show isotropic FSs. In contrast, in the 50 nm wires, the periods for both the S and BL sequences are highly anisotropic. This is shown in Fig. 2; i.e., for 50 nm wires, the LMR ($\theta = 0^\circ$) does not exhibit oscillations while the MR for $\theta = 15^\circ$ does. The existence of BL states and the observation of a large MR anisotropy in the 50-nm case, where $\lambda_F \sim d$, is consistent with the observations, using infrared-absorption (IR) spectroscopy, of low-effective-mass electrons and holes molded by quantum confinement including quantum interference around the wire.¹⁴

Consistent with our identification of the observed resonances with 3D Landau-level crossings through the Fermi level, it is appropriate to consider them as quasiparticles and we index the S and BL peaks with the integers N_S and N_{BL} that represent tentative occupation numbers [Fig. 3]. Behnia's resonances data were also included in Fig. 3. The data are roughly consistent with an expectation of constant slopes. Remarkably, we find that the nanowires data for the S sequences and Behnia results are similar in slope and therefore in FS cross-sectional area, strongly suggesting a commonality for the Fermi surface of the boundary layers from which the peaks originate.

We next considered whether the presence of surface carriers as observed in the present Rapid Communication for nanowires is responsible for the unusual results observed via the Nernst coefficient measurements³ for bulk Bi. It is already known that the mean-free path of holes is long, probably exceeding the lateral dimension of the sample. The re-

sults in Fig. 3 suggest that the carriers in the bulk, whose current is measured at the end of the sample, experience significant energy relaxation by interaction with surface states. In that case, the thermoelectric potentials would exhibit resonances in magnetic fields where the surface states cross the Fermi level.

Our data extend only to 0.07 T^{-1} . Assuming that Behnia's data arose from surface-state LS, the range of observation is smoothly extended to 0.03 T^{-1} . The true quantum limit is reached when the extrapolation of data in Fig. 3 crosses the abscissa which can be estimated to be 0.015 T^{-1} or $\sim 70 \text{ T}$. The quantum limit for the 30-nm-BL sequence is found to be 8.3 T , which is not very different from the quantum limit of the holes in bulk Bi.

The periods in Fig. 3 are significant considering that Bi is a compensated conductor where—because of charge neutrality—the sum of densities of positive and negative charges is zero for all values of H . This effect causes Fermi-level dependences upon H near the quantum limits.¹⁷ If we consider our interpretation of Behnia's data as evidence of surface-state LS, it is not surprising that period changes are observed near the S quantum limit ($N_S \rightarrow 0$). This is evidence that the Fermi energy in the surface layer has shifted to a position significantly lower than that in the bulk. The existence of this Fermi-level bending makes it less surprising that period changes are not observed near the hole, or BL for that matter, quantum limit and that $n_{\text{BL}} \sim 1/3n_0$, even though 30 nm nanowires are on the SC side of the SMSC transition ($E_c > E_0$). Charge neutrality may even play a role in place of or in addition to the quantum-mechanical hybridization for bulk carriers-surface-states energy relaxation in Bi. Further analysis of the LS spectroscopic results and theoretical study is required to gain deeper understanding.¹⁹

Our interpretation may explain the results by A. Banerjee *et al.*²⁰ They report observing no sharp resonances in BiSb alloys. Because BiSb has a much shorter electronic mean free path than Bi, the thermopower of BiSb is diffusive in origin and is therefore much less dependent upon surface state dynamics than that of Bi.

To summarize, we investigated electronic magnetotransport in small-diameter trigonal Bi wires. Landau states consistent with high-effective-mass quasiparticles (S) formed from the surface states in a boundary layer tens of nanometers thick are observed to be associated with a 3D Fermi surface. In the finer wires that are on the semiconductor side of the SMSC transition, low-effective-mass bulklike (BL) quasiparticles are observed with densities comparable to the densities of electrons and holes in the bulk. The BL properties are reminiscent of those observed with IR. In the large-diameter nanowires, holes, Dirac electrons, and S quasiparticles coexist. Our assignments are made by comparing properties that we observe with those of the BL and S features as observed with IR in nanowires and ARPES in films. We conclude that the unusual resonances that are observed in the Nernst coefficient of bulk Bi at high magnetic fields are evidence of energy relaxation between S quasiparticles and ballistic holes rather than a signature of charge fractionalization. It is anticipated that S quasiparticles will become as essential as Dirac electrons and holes in describing the state of Bi between the hole quantum limit at 9 T and the S quantum limit at around 70 T .

ACKNOWLEDGMENTS

Our work was supported by the Division of Materials Research of the U.S. National Science Foundation.

¹N. Miura, K. Hiruma, G. Kido, and S. Chikazumi, *Phys. Rev. Lett.* **49**, 1339 (1982).

²M. P. Vecchi, J. R. Pereira, and M. S. Dresselhaus, *Phys. Rev. B* **14**, 298 (1976).

³K. Behnia, L. Balicas, and Y. Kopelevich, *Science* **317**, 1729 (2007).

⁴L. Li, J. G. Checkelsky, Y. S. Hor, C. Uher, A. F. Hebard, and N. P. Ong, *Science* **321**, 547 (2008).

⁵R. B. Laughlin, *Phys. Rev. Lett.* **50**, 1395 (1983).

⁶A. Huxley and A. G. Green, *Science* **317**, 1694 (2007).

⁷R. Hartman, *Phys. Rev.* **181**, 1070 (1969).

⁸N. W. Ashcroft and N. D. Mermin, *Solid State Physics* (Harcourt Brace College, New York, 1976), Chap. 14, p. 258.

⁹P. Hofmann, *Prog. Surf. Sci.* **81**, 191 (2006).

¹⁰T. Hirahara, T. Nagao, I. Matsuda, G. Bihlmayer, E. V. Chulkov, Y. M. Koroteev, P. M. Echenique, M. Saito, and S. Hasegawa,

Phys. Rev. Lett. **97**, 146803 (2006).

¹¹T. E. Huber, K. Celestine, and M. J. Graf, *Phys. Rev. B* **67**, 245317 (2003).

¹²T. E. Huber *et al.*, *Appl. Phys. Lett.* **84**, 1326 (2004).

¹³V. B. Sandomirskii, *Sov. Phys. JETP* **25**, 101 (1967).

¹⁴M. R. Black *et al.*, *Phys. Rev. B* **68**, 235417 (2003).

¹⁵L. M. Roth and P. N. Argyres, in *Semiconductors and Semimetals*, edited by R. K. Willardson and A. C. Beer (Academic Press, New York, 1966).

¹⁶Z. B. Zhang, X. Sun, M. S. Dresselhaus, J. Y. Ying, and J. Heremans, *Phys. Rev. B* **61**, 4850 (2000).

¹⁷G. E. Smith *et al.*, *Phys. Rev.* **135**, A1118 (1964).

¹⁸A. Nikolaeva, D. Gitsu, L. Konopko, M. J. Graf, and T. E. Huber, *Phys. Rev. B* **77**, 075332 (2008).

¹⁹J. Alicea *et al.*, arXiv:0810.3261v1 (unpublished).

²⁰A. Banerjee *et al.*, *Phys. Rev. B* **78**, 161103 (2008).